TEKTONIKA

Quantitative Analysis of Natural Fracture Networks in Maastrichtian Chalk: Insights from a 7,000 m^2 Digital Outcrop Model of the Rørdal Quarry, Denmark

Tala M. Aabø *[1], **Simon J. Oldfield** [2,3,4], **Lars Stemmerik** [2], **Lars Nielsen** [2]

[1]Department of Geosciences and Natural Resource Management, University of Copenhagen, Copenhagen, Denmark | [2]Geological Survey of Denmark and Greenland, Copenhagen, Denmark | [3]Geo, Kongens Lyngby, Denmark | [4]School of Earth and Environment, University of Leeds, Leeds, United Kingdom

Abstract This study presents a comprehensive analysis of over 27,400 individual fractures from a digital outcrop model (DOM) of Maastrichtian-age chalk in the Rørdal Quarry, northern Jutland, Denmark. The extensive dataset, covering approximately 7,000 square meters, provides a detailed mapping of fracture networks representing a more extensive and continuous area than traditional scanlines and smaller aerial sampling methods. Analysis reveals significant spatial variations in fracture orientations and lengths, influenced by local fault systems and regional tectonics within the Sorgenfrei-Tornquist Zone (STZ). The resulting fracture network supports anisotropic fluid flow, with NE-oriented extensional fractures serving as primary pathways and NW-NNW and NNE-oriented shear fractures enhancing connectivity. Comparisons with other Danish chalk quarries, such as Sigerslev, Hillerslev, and Nye Kløv, highlight both similarities in regional trends and local variations due to factors like salt tectonics. The fractures in Rørdal exhibit a log-normal spacing distribution across the quarry, indicating a regularly spaced pattern. These findings underscore the potential of using outcrop analogues to inform subsurface models, particularly for predicting anisotropic fluid flow. However, careful consideration is required when applying outcrop data, ensuring that variations in fracture connectivity, stress regimes, and scale-dependent characteristics are accurately integrated to optimize carbon storage strategies and other subsurface applications.

Executive Editor:
Tony Doré
Associate Editor:
Noah Phillips
Technical Editor:
Mohamed Gouiza

Reviewers:
Haakon Fossen
Roy H. Gabrielsen

Submitted:
8 August 2023
Accepted:
4 December 2024
Published:
11 March 2025

1 Introduction

Upper Cretaceous chalk in NW Europe represent economically important reservoirs, characterized by high porosity and low permeability (*Bonto et al.*, 2021). These reservoirs often exhibit some degree of permeability anisotropy, influenced by fracturing (*Bisdom et al.*, 2017). This study examines the natural fracture network in Maastrichtian-age chalk at the Rørdal Quarry in northern Jutland, Denmark. Understanding the spatial distribution and geometry of sub-seismic scale fractures is crucial for optimising fractured reservoir development (*Anderson and Thunvik*, 1986; *Andreo et al.*, 2008; *Petrella et al.*, 2015).

Outcrops are the only reliable source for studying fracture networks at reservoir scale. Subsurface modelling of sub-seismic fractures is challenging due to reliance on well data, which inadequately captures spatial variability, as wells typically penetrate less than 1% of the reservoir area (*Howell et al.*, 2014; *Welch et al.*, 2020). Moreover, natural fracture networks are multiscale systems formed through complex processes that are difficult to replicate computationally or in laboratory settings (*Bisdom et al.*, 2017).

The Rørdal Quarry is considered an onshore analogue to over-pressured North Sea chalk reservoirs, particularly in the shallower parts of the offshore succession (*Jakobsen and Madsen*, 1997; *Aabø et al.*, 2020), apart from a lower degree of diagenesis (*Odling et al.*, 1999). Understanding the fracture network at Rørdal can improve subsurface fracture models (*Bisdom et al.*, 2017; *Cawood et al.*, 2017). Evaluating the spatial variability and anisotropy of fracture systems, and their contribution to subsurface models, depends on the fracture dataset's size, trace size range, and sampling methods (*Bonnet et al.*, 2001; *Bisdom et al.*, 2017; *Ortega et al.*, 2006). Limited outcrop data can lead to inaccurate subsurface fracture and fluid flow models (*Watkins et al.*, 2015).

We developed a comprehensive fracture dataset of over 27,400 traces, mapped on a digital outcrop model (DOM) covering a 1 km long and 7-10 m high section of the Rørdal Quarry wall, with approximately 7,000

*✉ tala@ign.ku.dk

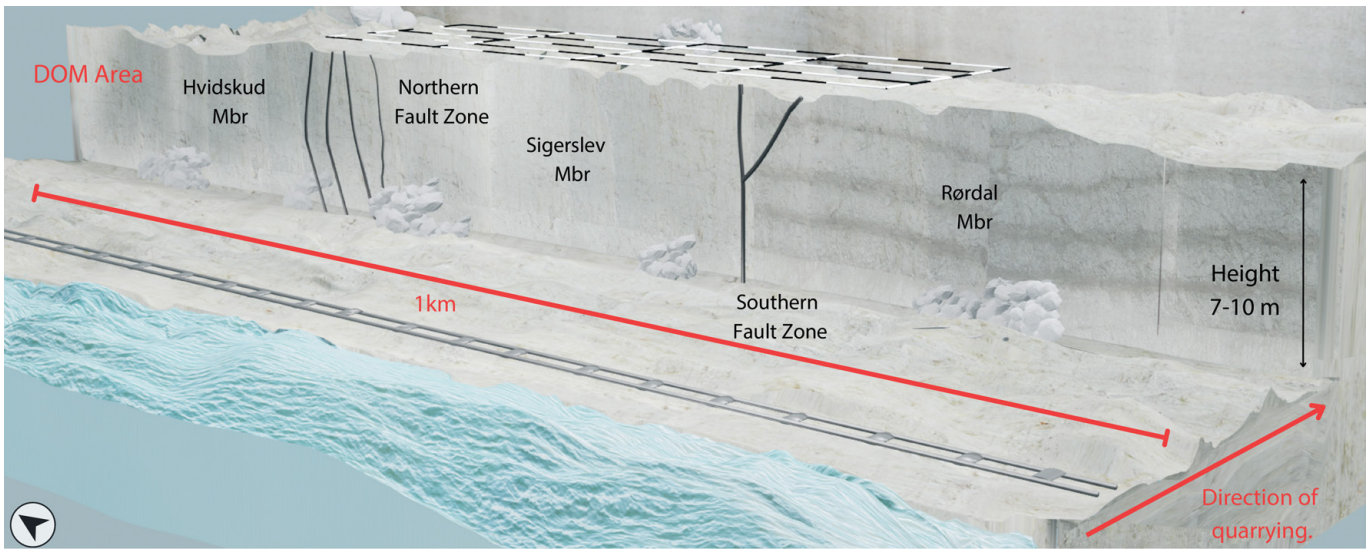

Figure 1 – 3D schematic illustration of the Rørdal Quarry showing main fault zones described by *Aabø et al.* (2023), the location of the three lithological units exposed at the quarry, the location of the digital outcrop model and the direction of quarrying from west to east.

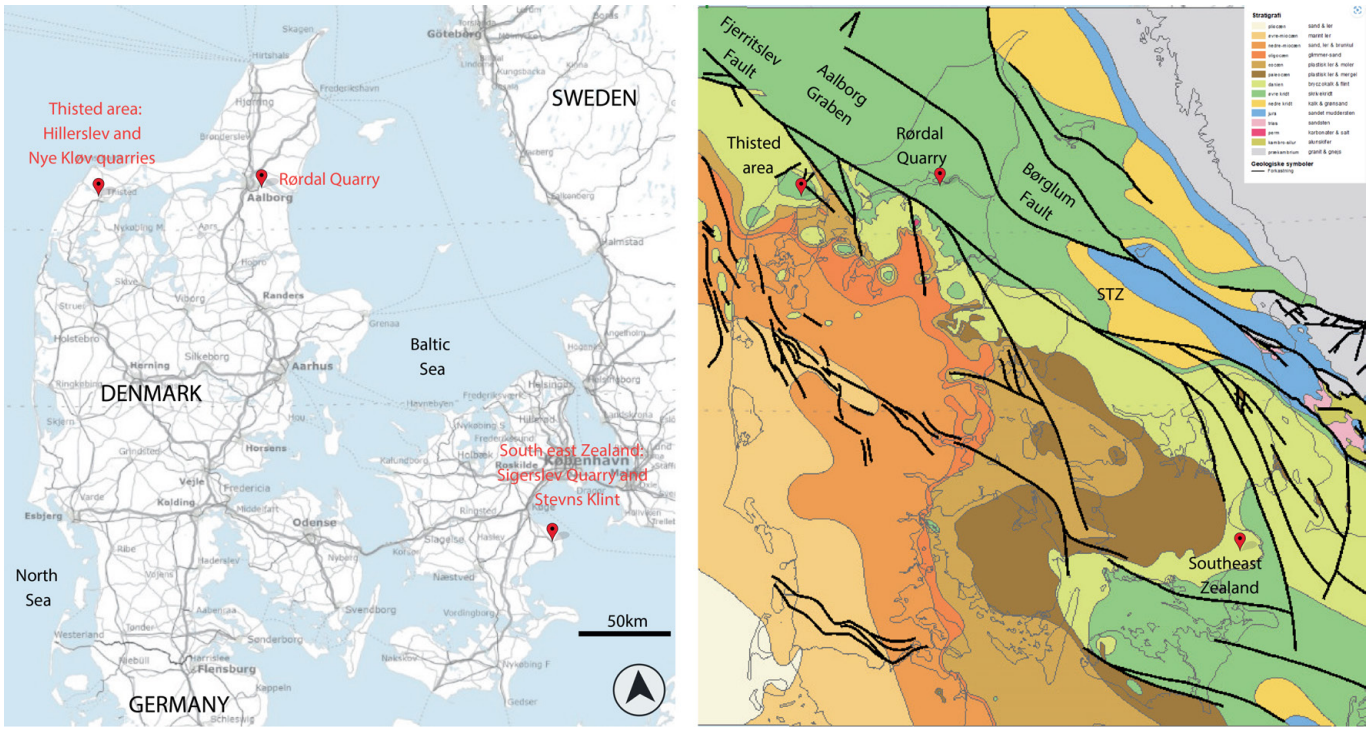

Figure 2 – Location of the Rørdal Quarry (left), situated in the Aalborg Graben, within the NW-SE trending Sorgenfrei-Tornquist Zone, approximately equidistant from the major boundary faults, the Fjerritslev and Børglum Faults (right). The location of the Hillerslev, Nye Kløv, Sigerslev and Stevns Klint chalk exposures are also indicated (based on *GEUS*, 2023).

square meters analysed in this study (Figures 1 and 2). The quarry has been in operation since 1889. The North-South oriented working face is currently being excavated eastwards at a rate of 20-30 m per year. As a result, fracture mappings at different times reflect the quarry wall's eastward progression. This ongoing excavation provides an opportunity to study the three-dimensional geometry of distinct fracture populations, providing insight into the evolution of the local stress regime at the time of fracturing. We compare fracture orientations measured in 1994/1995 during the Joule II programme (*Madsen*, 1995; *Odling et al.*, 1999), in 2016 (DOM dataset), and in 2023 (field measurements from this study). Figure 3 illustrates the relative positions of the quarry wall over time from 1995 to 2023.

Odling et al. (1999) noted that the Joule II data collection, based on scanlines and limited aerial sampling, was restricted to quarry surfaces, inherently limiting the scale of analysis. In contrast, our extensive dataset, representing large-scale aerial sampling, enables a more detailed and comprehensive analysis of the

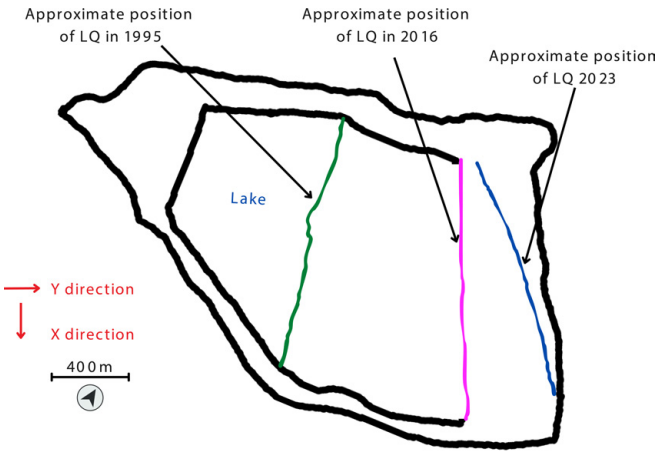

Figure 3 – Positions of quarry wall in 1995 (left), 2016 (middle) and 2023 (right), subjected to fracture mapping in 1995, 2016 and 2023, respectively, according to historical data from Google Earth dated 1995, 2015 and 2022. At the time of the Joule II program, the exposed section was about 1100 m long. As exposed in 2016 and in 2023, the quarry section is about 1000m long.

fracture network, improving predictions of subsurface fracture behaviour and fluid flow in similar chalk reservoirs. We observe fracture characteristics from millimetre to metre -scale fractures across multiple grid blocks, and their expected impact on fluid flow. A theoretical background on fracture attributes, distributions, and their relation to fluid flow is provided in the Appendix. I

Larger-scale structural features are constrained based on a time series of digital outcrop models, integrated with shallow seismic and ground penetrating radar (GPR) data, as described by *Aabø et al.* (2023). The composite geological model provides high-resolution, three-dimensional views of the main structural elements present in the Rørdal Quarry. In this paper, we expand on the previously published structural framework by providing a more detailed analysis of the local fault zones and their influence on the fracture network.

Finally, we compare our findings with published fracture data from other Danish chalk outcrops including examples inside and outside salt-influenced domains.

2 Study Area

The Rørdal Quarry is located within the Aalborg Graben, along the northern margin of the Danish-Norwegian Basin, and lies between the Fjerritslev and Børglum Faults (Figure 2). The region is part of the Sorgenfrei-Tornquist Zone (STZ), a significant fault zone separating the Scandinavian craton from the Danish-Norwegian Basin. The STZ has experienced multiple phases of tectonic activity, particularly during the Late Cretaceous and Early Palaeogene, when regional stress reorientations led to the inversion of older depocenters and extensive erosion of chalk formations (*Erlström and Sivhed*, 1981; *Ziegler*, 1990; *Egebjerg Mogensen and Korstgård*, 2003).

The chalk sequence at Rørdal Quarry is relatively thin, with a stratigraphic thickness of approximately 110 metres, comprising of three Maastrichtian-age lithological units. The Hvidskud Member, the oldest, consists of clean white chalk with scattered flint nodules. Above it lies the Rørdal Member, characterized by interbedded marl and marly chalk, with alternating layers of pure chalk and chalk with higher insoluble residue content. The uppermost unit, equivalent to the lower part of the Sigerslev Member in eastern Denmark, contains scattered marl beds and flint bands (Surlyk et al., 2010; Surlyk et al., 2013). Chalk porosity ranges between 42% and 50%, with matrix permeability varying from 4 to 20 mD (*Jakobsen and Madsen*, 1996). The section's maximum burial depth was approximately 450-600 meters (*Nielsen et al.*, 2011).

The quarry is actively excavated at a rate of 20-30 m per year, moving eastward. Two major fault zones—a northern NE-SW striking normal fault zone with SE-dipping faults, and a southern strike-slip fault zone also striking NE-SW—along with observed symmetric E-W oriented open folds, play a significant role in the spatial distribution and geometry of the fracture network within the quarry (*Aabø et al.*, 2023). This structural configuration was derived from a composite geological model, integrating digital outcrop models, ground-penetrating radar and shallow seismic data (*Aabø et al.*, 2023, Figure 2). The associated structural features were observed in both the 2016 and 2023 quarry configurations, corresponding to the positions of the quarry walls at those times. The fracture mappings presented in this paper are based on these configurations, reflecting the changes in the excavation over time (Figure 3). An expanded analysis of the fault zones and their structural features, established by *Aabø et al.* (2023) is given in the result section of this paper.

The chalk exposures considered in this study feature pronounced horizontal fractures, typically extending up to 20 meters in length, which segment the chalk into distinct mechanical layers. *Jakobsen and Madsen* (1996) found that the steeply dipping fractures were in some cases displaced by the horizontal fractures in the Rørdal Quarry, indicating a cross-cutting relationship. These near-bedding parallel features are commonly observed in Danish chalk outcrops, alongside numerous vertical fractures that vary in scale from millimetres to metres (*Rosenbom and Jakobsen*, 2005). Alternate mechanisms have been proposed for the formation of these horizontal fractures, including a horizontal shear traction beneath glaciers coupled with over-pressurized basal meltwater (*Boulton and Caban*, 1995); stress release response during Neogene uplift (*Rosenbom and Jakobsen*, 2005); or, glacial unloading induced horizontal relaxation-fracturing (*Jakobsen and Madsen*, 1996; *Frykman*, 2001).

3 Fracture Mapping and Structural Analysis in Rørdal Quarry: Joule II Insights

Structural elements and fracture attributes in the Rørdal Quarry were mapped as part of the Joule II program of the European Commission (CT93 0334) in 1994 and 1995 (*Madsen*, 1995; *Odling et al.*, 1999). Fracture lengths and orientations were measured within three one square metre areas on vertical sections of the lower quarry wall. Fracture spacings were estimated using scanlines ranging from 10 to 31 m in length. The orientations measured in 1995 indicate a dominant fracture strike in the NW-NNW direction, reflecting the primary stress orientation at the time of fracturing, with a secondary perpendicular fracture set striking NE-SW. In the Joule II program, mapped joints in the Rørdal Quarry follow log-normal trace length distributions. Fracture spacings in horizontal line samples show a range from clustered to anti-clustered, with a variation coefficient (C_v) ranging from 0.6 to 1.3. The variation coefficient is a measure of spacing variability, where values closer to 0 indicate uniform spacing, while higher values suggest more variability, ranging from clustered ($C_v < 1$) to anti-clustered ($C_v > 1$) distributions. On average, the distribution is described as random. The connectivity of the fracture patterns in the one square metre areas was described as high, as dead ends constitute only a small portion of the system.

4 Comparative Geological Background of Additional Quarries

4.1 Sigerslev Quarry

The Sigerslev Quarry is situated within the Danish Basin, which is part of the Sorgenfrei-Tornquist Zone, and exposes Maastrichtian-age chalk similar to that found at the Rørdal Quarry. Both quarries have complex fracture networks shaped by regional tectonic activity during the Late Cretaceous and Early Paleogene. At Sigerslev, the fracture network is particularly influenced by the tectonic setting within the Sorgenfrei-Tornquist Zone (STZ), where dextral strike-slip faulting and regional uplift have been key in fracture formation. The fracture system at Sigerslev comprises four primary sets of vertical fractures with strikes at 25°, 60°, 145°, and 175°, similar to those identified at the Rørdal Quarry, indicating a consistent regional stress regime. These orientations align with the regional stress directions, where the maximum stress (σ_1) is oriented NE-SW, consistent with the tectonic forces associated with the STZ and observed at both the Sigerslev and Rørdal quarries. The NE-SW striking faults observed at both the Sigerslev and Rørdal quarries suggest not only a shared tectonic history but also similar responses to the regional stress fields imposed by the STZ during the Late Cretaceous and Early Paleogene. The chalk at Sigerslev exhibits a porosity ranging between 45% and 50%, with a matrix permeability of approximately 8×10^{-15} m^2 (*Rosenbom and Jakobsen*, 2005).

4.2 Hillerslev Quarry

The Hillerslev Quarry, which exposes Maastrichtian chalk, is located in the eastern half of the Thisted Dome, an area characterized by salt-induced structural highs, which influence the distribution and orientation of fractures in the region. The general tilt in the area is approximately 4° towards the ESE, with chalk layers exhibiting low diagenetic alteration, retaining high porosity values of 44% to 52% and matrix permeabilities ranging from 5.1 mD to 13.4 mD.

Fractures in Hillerslev Quarry are widely scattered, with predominant strike orientations of ENE-WSW and NNW-SSE. Most fractures are steeply dipping, with a dominance of almost vertical fractures. The dip direction is primarily towards the E and SE, reflecting the regional stress influence of the Thisted Dome's structural configuration. The fracture density is described as close to random, with a coefficient of variation ranging from 0.8 to 0.9, indicating a tendency towards anti-clustered spacing (*Thrane and Zinck-Jørgensen*, 1997).

4.3 Nye Kløv Quarry

The Nye Kløv Quarry is situated in the eastern part of the Thisted Dome, within a postglacial fault-generated sea cliff. The quarry exposes both Maastrichtian and Danian chalk, with the Maastrichtian chalk being a burrowed massive chalk mudstone, while the Danian sequence is characterized by a gradual increase in bryozoan content, culminating in a few meters of bryozoan limestone. The general tilt of the sequence is towards the E, away from the center of the dome, with the Maastrichtian/Danian boundary marked by a thin, light-grey marl layer.

Fractures in Nye Kløv Quarry exhibit two dominant orientations: NNE-SSW and NW-SE. The majority of fractures are steeply dipping, with vertical to near-vertical dips. The dip direction of the NNE-SSW striking fractures is predominantly towards the ESE, while the NW-SE striking fractures dip almost equally towards the NE and SW. These orientations are consistent with the overall structural influence of the Thisted Dome (*Thrane and Zinck-Jørgensen*, 1997).

5 Methodology

5.1 3D Fault Analysis

The composite geological model, published in *Aabø et al.* (2023), combines a time series of digital outcrop models (DOMs) with GPR and shallow seismic data to create a high-resolution, three-dimensional representation of the geological features in the Rørdal Quarry. Data for the DOM time series were collected in 2016, 2018 and 2019, reflecting the positions of the quarry wall at the different times. A total of 1261 high-resolution images were captured in 2016 using a Nikon D800E DSLR camera. For subsequent years, UAV flights with a DJI Matrice 210 were employed to collect imagery. These images were georeferenced using the UAV's built-in RTK module. The data from these

surveys were processed using Structure-from-Motion (SfM) photogrammetry and multi-view stereo (MVS) techniques in Agisoft Metashape Pro, generating dense point clouds, meshes, and textures. Full details on the processing of the individual datasets and the integration of the shallow geophysical data with the DOM time series are provided in *Aabø et al.* (2023).

5.2 Data Collection and Digital Outcrop Modeling

5.2.1 Fracture Mapping Approach

The fracture data presented in this paper are based on the DOM of the quarry's position in 2016, supplemented by hand measurements taken in 2023. Fracture traces of all sizes within the resolution limits of the digital outcrop model were sampled along the full 1 km length and 7-10 m height of the exposed chalk section in Rørdal. Using the Compass plugin (*Thiele et al.*, 2017) in CloudCompare (*Gim*, 2016), fractures were mapped based on least-cost paths between user-defined nodes, following dark points in the cloud. The full workflow for data processing and mapping is highlighted in Figure 4.

5.2.2 Fracture Trace Characteristics

The dataset captures mm to meter-scale fractures, though some mm-scale fractures may be truncated due to resolution limits (*Aabø et al.*, 2023), and the true lengths of fractures extending beyond the mapped area remain unknown. Approximately 3,000 near-horizontal, bedding-parallel fractures, which are likely the result of near-surface processes such as glaciation-related shear and post-glacial rebound, were excluded from this study. This exclusion was made to focus on tectonic fractures relevant to subsurface fluid flow and reservoir behaviour.

5.3 Fracture Analysis Techniques

5.3.1 Structural Attributes and Spacing Analysis

Fracture traces were analysed as polylines in both 3D and 2D, with X, Y, Z coordinates recorded for each node. Using the method of *Ortega et al.* (2006), fracture spacings were sorted, numbered, normalized by the 1,000 m length of the quarry wall, and plotted to obtain a graphical representation of their distribution and best-fit distribution for various spacing ranges.

5.3.2 Fracture Orientation Analysis and Comparative Assessment across Danish Chalk Outcrops

Fracture strikes were estimated using x, y, z coordinates, with a straight line drawn approximately north to south. Variations in y-coordinates, primarily due to quarrying-induced wall fluctuations, resulted in most strike estimations being marked as low confidence. Higher confidence estimations were made where y-coordinate variations reflected actual geology.

The progressive eastward excavation of the Rørdal Quarry since 1889 allowed us to study the variations of the local stress field by comparing fracture orientations measured at different times and positions along the quarry wall. We compared orientations measured in 1995 (Joule II), 2016 (digital measurements from a DOM dataset), and 2023 (field measurements from this study), with additional constraints from 49 hand measurements of dip and dip azimuth taken in 2023.

To further assess along-strike variability, our findings were compared with findings from the Joule II programme, as well as measurements from the Hillerslev and Nye Kløv quarries, which are located in areas impacted by salt diapirism. This broader comparison provided insights into orientation distributions across Danish outcrops and highlighted the effects of salt tectonics on fracture patterns.

5.4 Advanced Fracture Attribute Analysis

5.4.1 Conversion and Analysis Using FracPaQ

The CloudCompare dataset was converted from 3(2.5)D to 2D for use in FracPaQ, a MATLAB toolbox for 2D quantification of fracture patterns (*Healy et al.*, 2017). Using the Geoseer Python package, data were reprojected to a local grid aligned with the quarry's exposed working face, minimizing offset between the observation plane. The data format was transformed to match FracPaQ's input requirements, resulting in an array of fracture traces composed of segments delimited by nodes (Figure 5).

5.4.2 Fracture Length Distributions and Connectivity

Fracture length distributions were evaluated in FracPaQ using Maximum Likelihood Estimators (MLE), which allows for objective assessments of possible data distributions (*Rizzo et al.*, 2017). MLE analysis was performed by subdividing the data according to lithological units and into 100 m intervals to evaluate variations in fracture length distribution. To analyze smaller (below 0.2 m) and larger (above 3 m) fractures, the data were further plotted in Excel using the same method as for fracture spacing analysis.

5.4.3 Fracture Intensity and Density Mapping

Fracture intensity and density maps were generated in FracPaQ using the circular scan line sampling method, visualizing fracture frequency along the full height and length of the quarry section. The intensity map (P21) reflects variations in fracture trace length per unit area, while the density map (P20) indicates the number of fractures per unit area. High values of P21 and P20 suggest high connectivity, and the relative proportion of splay nodes to isolated nodes provided insights into potential flow pathways.

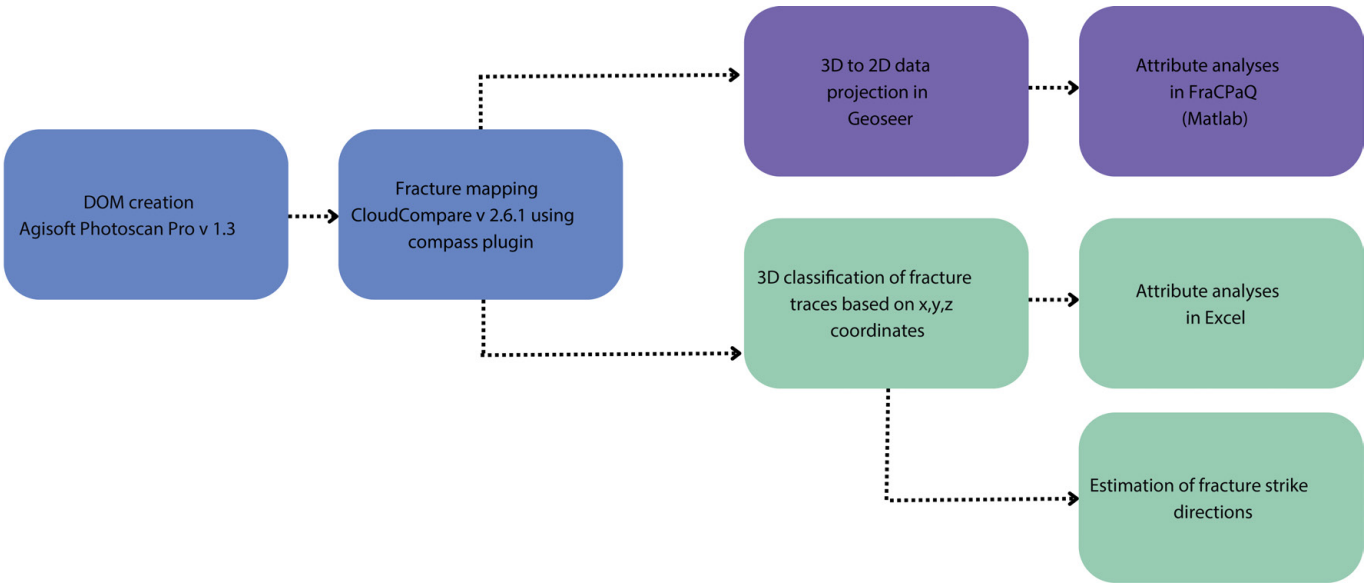

Figure 4 – Workflow for building extensive dataset of fracture traces in the Upper Maastrichtian fracture system exposed in the Rørdal Quarry, Northern Jutland. Blue boxes relate to the creation of the digital outcrop model and the mapping of individual fracture traces, purple and green boxes describe 2D and 3D analysis of the fracture dataset consisting of more than 27 400 fractures, respectively.

5.5 Considerations and Limitations

While active cement production at the Rørdal Quarry has reduced the impact of erosion on fracture apertures, the possibility of fracture reactivation during exhumation, despite the lack of abundant veins, means that current aperture measurements may not fully represent subsurface conditions. As a result, quantification of fracture apertures was excluded from this study.

The high-resolution digital outcrop model captures fractures ranging from millimetre to metre scale. As with other observation methods, fracture-length population distributions are expected to feature censoring (reduced count of shorter fractures, limited by the resolution of the survey) and truncation (reduced count of longer fractures, limited by the maximum length of fracture continuously visible across the area of observation). Near-horizontal fractures were excluded from analysis in this survey to focus on tectonic fractures more relevant to subsurface fluid flow. While this decision aligns with the study's objectives, excluding these fractures may limit the comprehensiveness of the overall fracture network analysis. The study also depends on fracture orientation data collected at different times and positions along the quarry wall, reflecting the quarry's progressive eastward excavation. This approach introduces variability due to both temporal changes and spatial variations in fracture patterns. The majority of strike estimations are marked as low confidence due to the shape of the quarry's working face, which impacts our orientation analysis accuracy. Comparisons with other Danish chalk outcrops, including those impacted by salt diapirism, offer a broader context but come with limitations. Differences in geological settings, lithology, and regional stress fields may affect the applicability of findings from Rørdal to other locations. The influence of salt tectonics introduces complexities absent in the Rørdal Quarry.

6 Results

6.1 Fault mapping

The Northern Fault is a normal fault zone, dipping southeast, juxtaposing the Hvidskud and Sigerslev members. It shows segmentation, with multiple SE-dipping faults and one NW-dipping splay fault, associated with a damage zone around 7 m wide and a throw of 5-10 m (*Aabø et al.*, 2023). The fault zone can be traced from the western to the eastern quarry sections, with a noticeable change in GPR penetration depth, marking the fault boundary. The fault plane shifts approximately 35 m northeast across the quarry (Figure 6).

The Southern Fault Zone marks the boundary between the Sigerslev and Rørdal members. It is a steeply dipping, segmented strike-slip fault, with offset segments (*Aabø et al.*, 2023). We do not have the data to constrain the relative movement of the fault blocks in the Southern Fault Zone. As the stratigraphically older Sigerslev Member appears before the stratigraphically younger Rørdal Member in the exposed section, there are two possible explanations for this. Either there is a left-lateral strike-slip movement, which requires a regional structural dip towards the west or there is a right-lateral movement, which requires a structural dip towards the east (Figure 7). The dip direction cannot be definitively determined from the available data, as it varies based on the position of the local folds. The fault is characterized by a flower structure, consisting of a SE-dipping planar segment and multiple splays. The Rørdal Member is distinguishable by its cyclic layers of lighter chalk and darker marl, while the Sigerslev Member is more homogeneous in appearance (Figure 8). The fault plane in the southern fault zone can be traced for about 60 m, dipping SE, with steeply dipping lineaments observed in the chalk section (Figure 9).

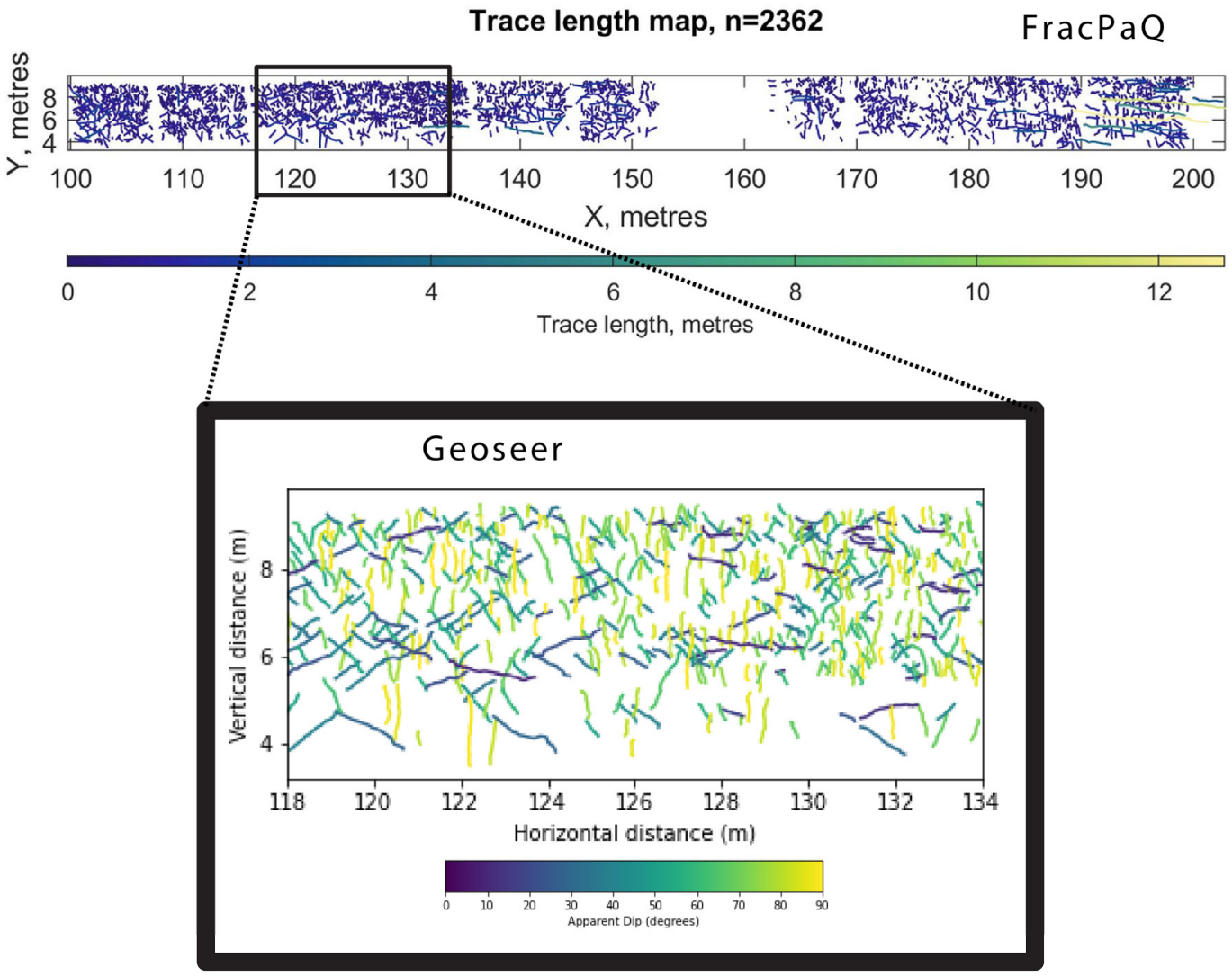

Figure 5 – Visualization of fracture traces in Geoseer (left) and FracPaQ (right) mapped in the Hvidskud Mb on DOM. The Geoseer data is color coded according to apparent dip and the FracPaQ data is filtered according to the total length of fracture traces. The Geoseer tool is used for optimizing input into FracPaQ according to the lithological unit and fracture attribute of interest.

6.2 Fracture Orientations and Dip Analysis in Rørdal Quarry

In the Rørdal Quarry, orientation data reveal spatial variations in dominant fracture trends from west to east across the quarry. In the western part (1995), the dominant fractures strike NW-NNW, with a secondary set oriented NE-SW. Moving eastward to the central part of the quarry (2016), the dominant orientation shifts to NNW, with a secondary NNE trend. By the easternmost section (2023), the dominant fracture orientation changes to NNE, while NW-NNW becomes the secondary set (Figure 10). These shifts likely reflect variations in fault influence across different sections of the quarry rather than changes in the overall regional stress regime. The 2016 stereonet contains only higher-confidence orientation data, but the observed strike distribution aligns with the full dataset.

The DOM data show predominantly steep dip angles, averaging 69° with a standard deviation of 19°. Most fractures (16,745) have dip angles between 70-90°, with shallower dips (below 30°) being less common. Dip distributions are consistent across the Hvidskud, Sigerslev, and Rørdal members, with the Hvidskud Member showing a slightly higher proportion of steep fractures.

Fracture length distribution analysis within the Hvidskud, Sigerslev, and Rørdal members shows average lengths of 0.52 m, 0.68 m, and 0.54 m, respectively (Figure 11). The Hvidskud Member is dominated by fractures in the 0.1-0.5 m range, while the Sigerslev and Rørdal members contain fractures primarily between 0.5-1.5 m. Large fractures (above 1 m) are rare across all units.

MLE analyses indicate that fracture trace length distributions are best described as log-normal. This pattern is consistent across 100m intervals along the quarry wall front (Figure 12).

Fracture intensity (P21) and density (P20) maps indicate higher fracture frequencies near the southern and northern fault zones (Figure 13). Average P21 values are 6.2 m^{-1}, 7.2 m^{-1}, and 7.0 m^{-1} for the Hvidskud,

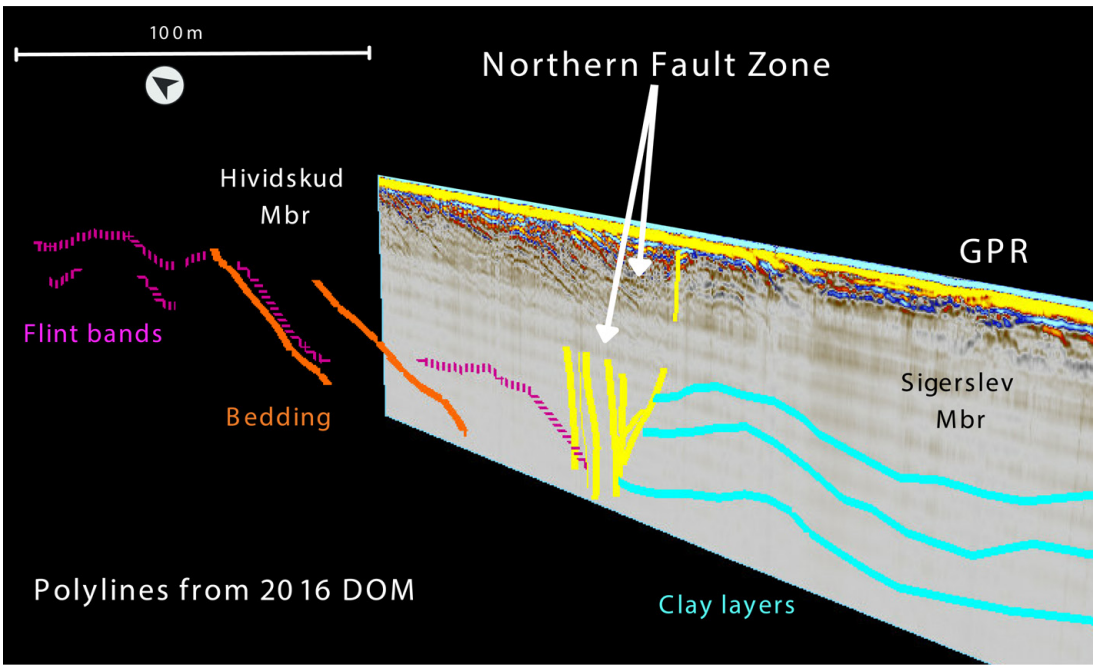

Figure 6 – The northern fault zone as observed in the composite geological model. In the GPR data the position of the northern fault zones is marked by a significant reduction in penetration depth between the Hvidskud Member (left/north) and the Sigerslev Member (right/south).

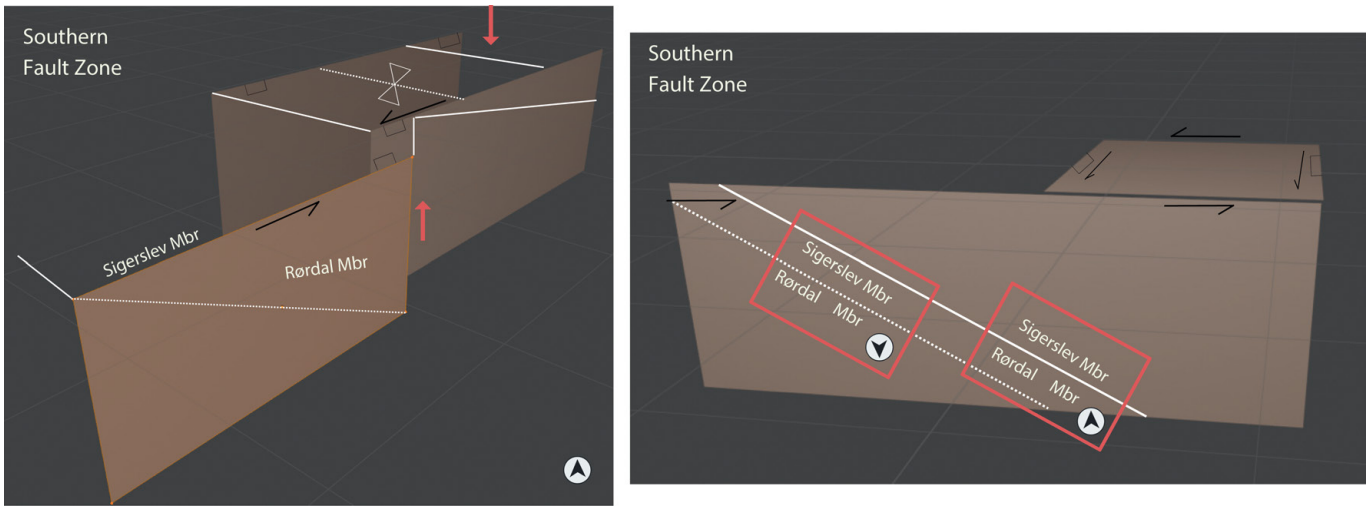

Figure 7 – Block diagram showing a possible model of the Southern Fault Zone, which is a strike-slip fault zone, juxtaposing the Sigerslev and Rørdal members.

Sigerslev, and Rørdal members, respectively. P21 is slightly higher near the Southern Fault Zone.

Fracture spacing, derived using the Ortega et al. (2006) approach, follows a log-normal distribution between 0.1 m and 1 m, with a log-log distribution for spacings below 0.1 m and above 1 m. The highest mean fracture spacing is found in the Rørdal and Sigerslev members, indicating slightly lower fracture densities compared to the Hvidskud Member. The variation coefficient ranges from 0.81 to 1.1, slightly lower than values reported in the Joule II programme, where C_v values were in the range of 0.6 to 1.3.

Fracture connectivity, as indicated by the distribution of isolated (I) and splay (Y) nodes, shows a high degree of connectivity across the quarry wall, with the highest concentration of splay nodes in the first 20 m of the Hvidskud Member, suggesting enhanced fluid flow potential in this region (Figure 14). Note that while the splay node acts as an indicator of fracture network connectivity, it does not separate between different fracture modes.

7 Discussion

The Rørdal Quarry is situated within the Aalborg Graben, along the northern margin of the Danish-Norwegian Basin, and is influenced by the broader tectonic framework of the Sorgenfrei-Tornquist Zone (STZ). Within the quarry, two local fault zones—the northern NE-SW striking normal fault and the southern NE-SW striking strike-slip fault—have played a significant role in shaping the spatial distribution and geometry of the fracture network.

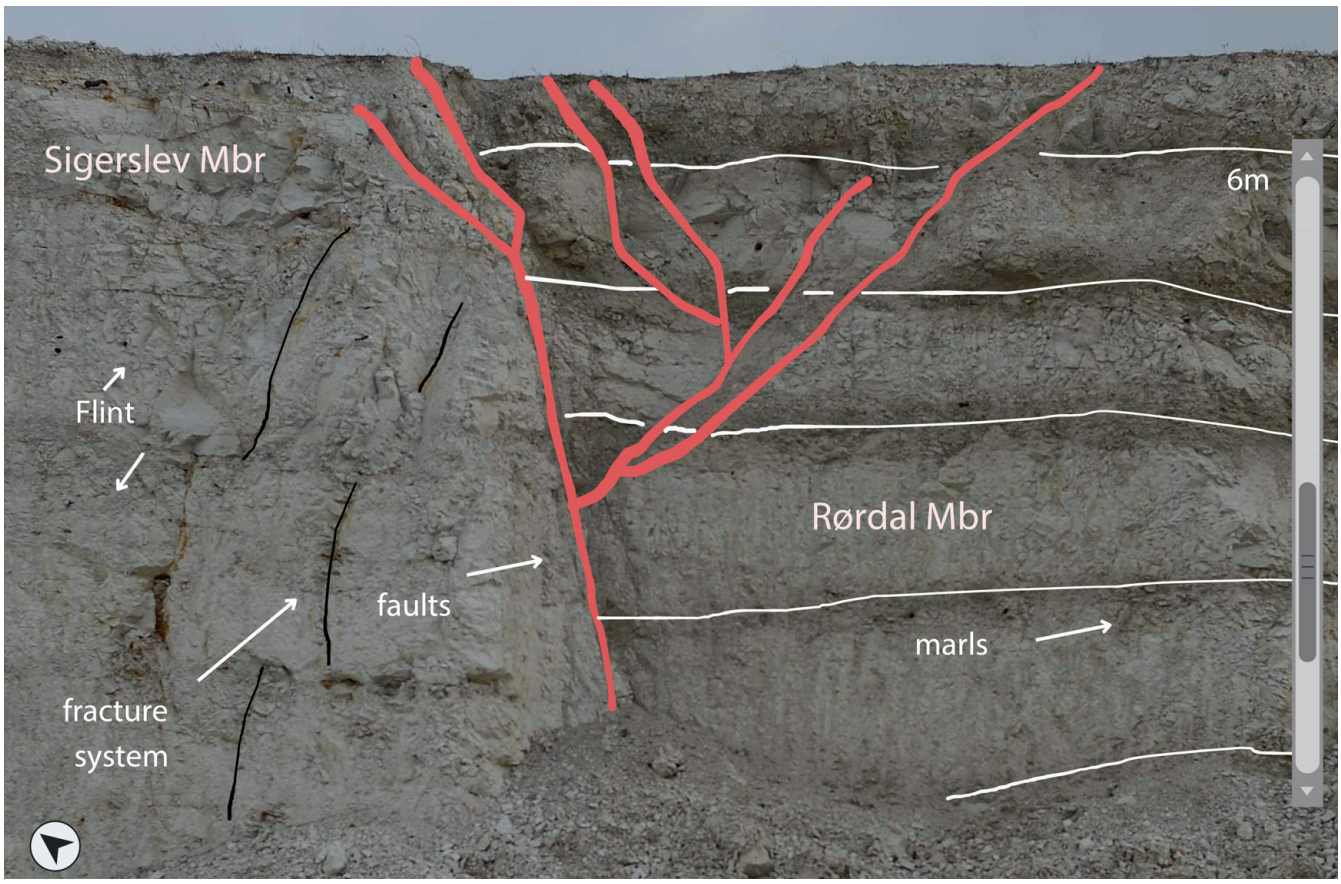

Figure 8 – Southern Fault Zone, as it appears in the digital outcrop model of the quarry as exposed in 2016.

The orientation of these faults aligns with the regional stress direction imposed by the STZ, contributing to the development of both shear and extensional fractures.

The northern NE-SW striking normal fault has predominantly influenced the formation of extensional fractures (NE-oriented). These fractures likely formed during an early phase of tensional stress, corresponding to a regional WNW-ESE stress orientation observed in the western quarry. As the tectonic regime evolved, shear fractures developed, oriented NW-NNW and NNE, influenced by the southern NE-SW striking strike-slip fault. This phase likely occurred under a compressional or transpressional stress regime, with the principal stress direction (σ_1) rotating to NNE-SSW moving eastward across the quarry.

The observed fracture zonation across the quarry reflects the interaction between these local fault systems and the regional stress field. The consistency of these dominant trends, as observed moving eastward across the quarry, suggests that while the primary stress regime remained stable during the overall period of fracture formation, deviations in fracture orientations are likely related to the influence of localised faulting. This deformation pattern is further supported by our findings on fracture length distributions, which vary across the lithological units. The largest fractures are found in the Rørdal Member, while shorter fractures dominate the Hvidskud Member, likely as a result of varying mechanical properties within the chalk.

Dip angles in the DOM data are well constrained, with an average dip of 69° and a standard deviation of 19°. Most fractures (64% of the population) have steep dips between 70-90°, while shallower dips below 30° are rare, constituting only 4% of the dataset. This consistency across different lithological units—Hvidskud, Sigerslev, and Rørdal members—suggests that the fracture network's structural attributes are largely controlled by regional tectonic forces, although local geological variations also play a role.

Fluid flow in the Rørdal Quarry is expected to be highly heterogeneous and anisotropic, with NE-oriented extensional fractures providing primary fluid pathways, while NW-NNW and NNE-oriented shear fractures contribute to varying degrees of connectivity. The steep dip angles of most fractures suggest strong vertical fluid migration, particularly in fault-dominated zones. Larger fractures in the Rørdal Member indicate higher permeability compared to the two other units. Subsurface models should account for these spatial variations in fracture connectivity, permeability, and stress regime influences to accurately predict fluid flow.

The Rørdal and Sigerslev quarries, unaffected by subsurface salt movements, display stress regimes influenced by regional tectonics and the Sorgenfrei-Tornquist Zone (STZ). Fracture orientations at these sites, while generally consistent with the regional stress directions, vary across Rørdal. To the West, NW-NNW fractures dominate, reflecting the influence of regional tectonics associated with the STZ during the earlier phase of fracturing. However,

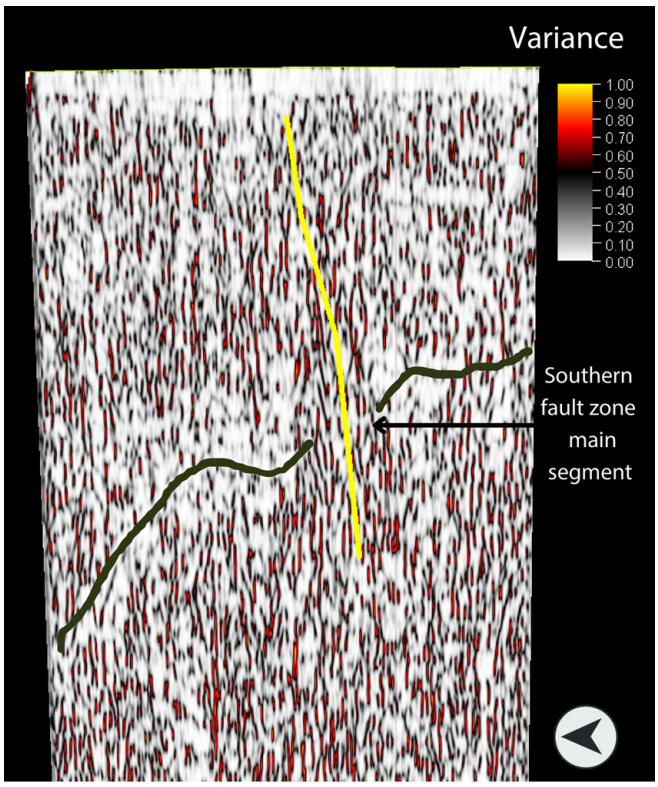

Figure 9 – Seismic attribute of shallow seismic 2D line, generated in Petrel using the structural edge enhancement workflow, showing full extent of southern fault zone and steeply dipping lineaments at depth. Red indicates lineament dips of 70-80°, which is in good correspondence with the observations at the surface.

towards the East, the dominant orientation shifts to NNE, particularly in the easternmost section recorded in 2023. This change suggests that while the regional stress regime imposed by the STZ was a significant factor, there were also localized influences that caused variations in fracture orientations across the quarry's spatial extent. The Sigerslev Quarry, on the other hand, shows a more consistent pattern with the regional stress directions, characterized by four primary fracture sets that align with the expected NE-SW orientation of the maximum principal stress, consistent with the dextral strike-slip faulting and regional uplift associated with the STZ.

This variation in fracture orientations at Rørdal, compared to the more uniform patterns observed at Sigerslev, suggests that while both quarries share a common tectonic history related to the STZ, Rørdal experienced additional localized stress influences from the two fault zones at the site, which altered the dominant fracture orientations over time.

In contrast, the Hillerslev and Nye Kløv quarries, which are impacted by salt tectonics associated with the Thisted Dome, display additional fracture sets striking NNW and NW. These orientations are indicative of the more complex stress fields that develop in regions affected by salt diapirism. The movement of salt structures can lead to significant reorientation of local stress fields, as the salt acts as a free surface, unable to support significant differential stress. In these settings fracture orientations are likely to appear to be misaligned with regional trends, as they form in response to more dominant local stress regimes, often orthogonal to interface between salt and deformed overburden material. These phenomena often present themselves as a more intricate pattern of fracturing that can include radial, concentric, and cross-cutting fractures, arranged around the upwelling salt geometry (*Zhang et al.*, 2024).

The steeply dipping lineaments observed in Rørdal are also prominent in the Thisted region's chalk exposures, particularly at Hillerslev Quarry. This consistency across multiple sites supports the interpretation of a regional tectonic influence on fracturing that may pre-exist halokinesis and be over-printed by later episodes of fracturing. These distinct features of salt-influenced and salt-free fracture patterns, highlight the importance of proper consideration of outcrop analogues in developing an understanding of likely fracture patterns in the subsurface. In this case an outcrop that may be less obviously analogous to a salt-influenced area provides useful insights into more subtle features that may be over-printed by later episodes of salt related deformation. Studying analogues that may represent an area of interest at different stages of its geological history may provide value in comparison to reservoirs with similar lithology, burial history and tectonic setting.

This study shows a meaningful difference between the extensive DOM data and the earlier data from the Joule II program, highlighting insights that smaller-scale studies may miss. The Joule II data, with C_v values ranging from 0.6 to 1.3, indicated that fracture spacing exhibited a mix of clustered and anti-clustered patterns, with a tendency towards greater variability and randomness across smaller, localized sampling areas. This broad range suggests a more heterogeneous fracture network, with zones of both regular and highly variable spacing. In contrast, the broader and more continuous dataset analysed in this study, with C_v values ranging from 0.81 to 1.1, reveals that fracture spacing follows a more uniform, log-normal distribution within the 0.1 to 1 m range across the entire 7,000 square meters of the quarry's working face. This narrower C_v range suggests a more consistent and slightly less variable spacing pattern, indicating that while localized variations in spacing still exist, the overall pattern across larger scales tends to be more regular.

The broader coverage of the DOM data also allowed us to detect higher fracture frequencies near the southern and northern fault zones and to observe a more uniform distribution pattern throughout the site. This consistency contrasts with the more varied and localised patterns observed in the Joule II data, particularly within the Hvidskud Member.

The main difference lies in the scale and extent of data collection. The Joule II data, although valuable, was limited by its smaller sampling areas, which led to a perceived variability in fracture patterns. However, DOM data provide a comprehensive view that captures the spatial variability and complexity of the

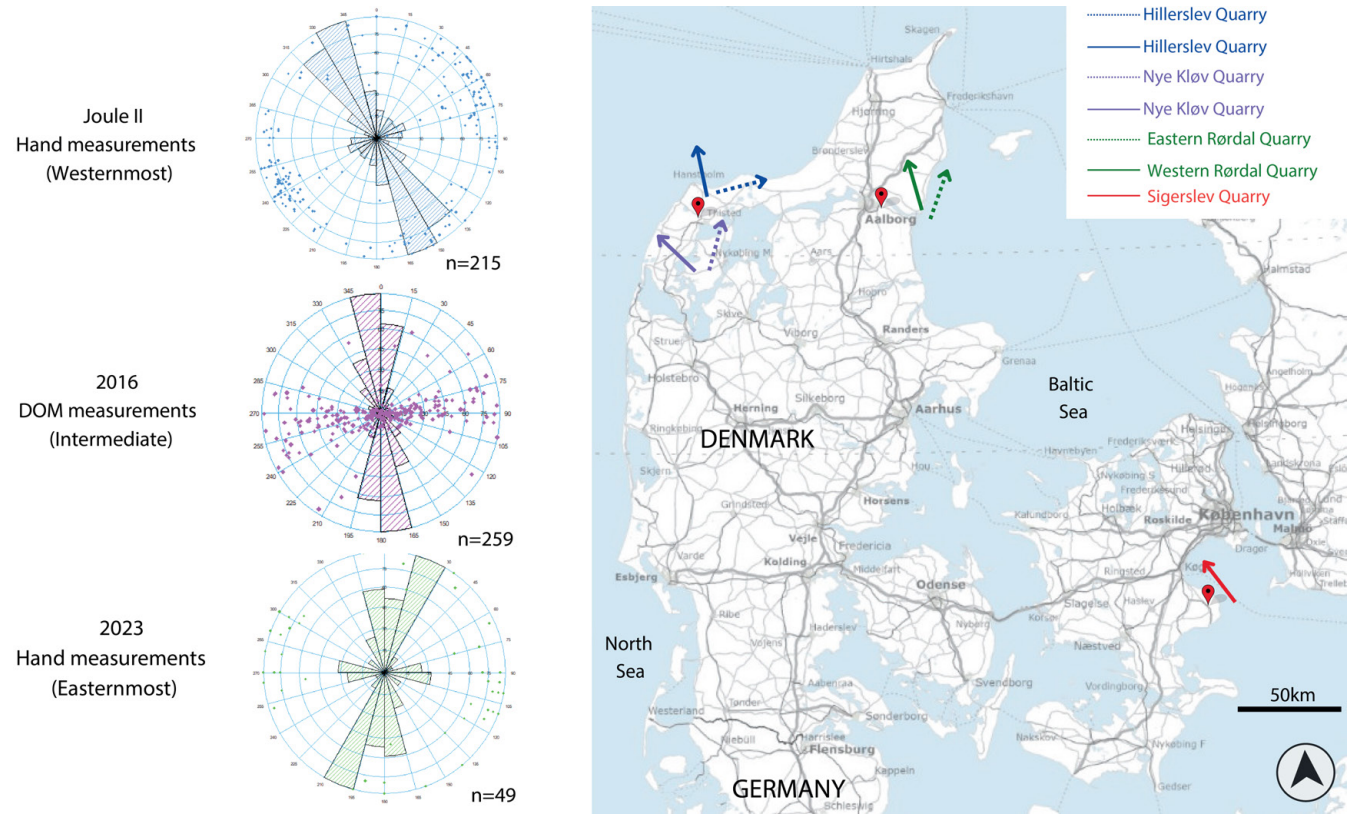

Figure 10 – Left: Fracture orientations of joints mapped in Rørdal quarry during Joule II program (*Madsen*, 1995), 2016 (estimated from best-fit to straight line approximation in this study) and 2023 (hand measurements from this study), showing dominating fracture trends striking NW-SE/ NNW-SSE, NNW-SSE and NNE-SSW, respectively. All stereonets represent dip and dip azimuth values and are overlain by strike rose diagrams. The plots were color-coded accorded to dataset and plotted in Petrel for the purposes of this study. Right: palaeo-stress directions (σ_3) in the Rørdal, Hillerslev, Nye Kløv and Sigerslev quarries – explored in the discussion.

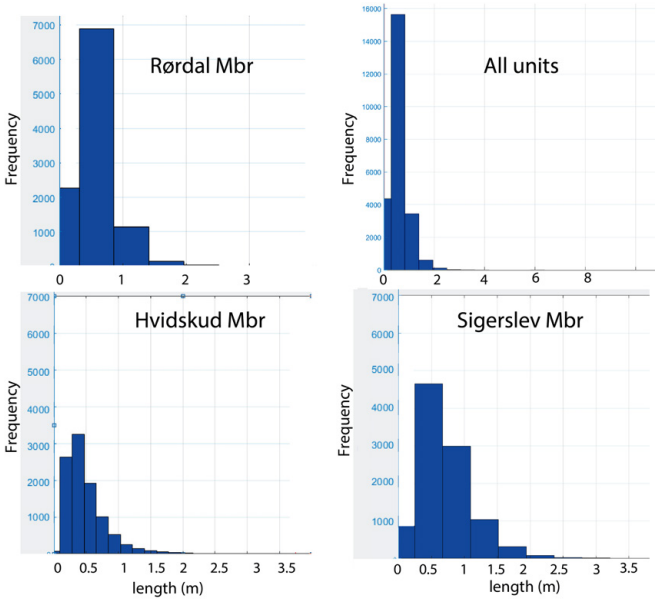

Figure 11 – Histograms showing the distributions of fracture trace lengths within each lithological unit and as a whole system, plotted in FracPaQ. The plots are based on mappings on DOM1A. When the system as a whole is considered, the vast majority of fractures have trace lengths between 0.3m and 1.3m. The relative proportion of shorter- and longer fractures occur in the Hvidskud and Rørdal members, respectively.

fracture network with greater precision. This extensive dataset not only supports the idea of a stable regional stress regime over time, but also highlights how local geological structures influence fracture orientations and connectivity.

These findings emphasize the importance of using large-scale, high-resolution datasets for geological studies, especially when predicting subsurface fluid flow and interpreting fracture networks. The comprehensive nature of the DOM data allows for a more accurate description of fracture systems, which is crucial for applications such as reservoir modelling and carbon storage. This study demonstrates that broader data collection efforts can lead to more reliable geological interpretations and better-informed decisions in subsurface resource management.

The connectivity of fracture patterns, as described in the Joule II program, indicated high connectivity with isolated fracture tips. This high connectivity is also reflected in our findings, particularly in the Hvidskud Member, where the fracture network appears well-connected, enhancing potential fluid flow. Fracture intensity (P21) and density (P20) maps show higher fracture frequencies near the southern and partially near the northern fault zones. The average P21 values for the Hvidskud, Sigerslev, and Rørdal members are 6.2 m^{-1}, 7.2 m^{-1}, and 7.0 m^{-1}, respectively, with P21 being

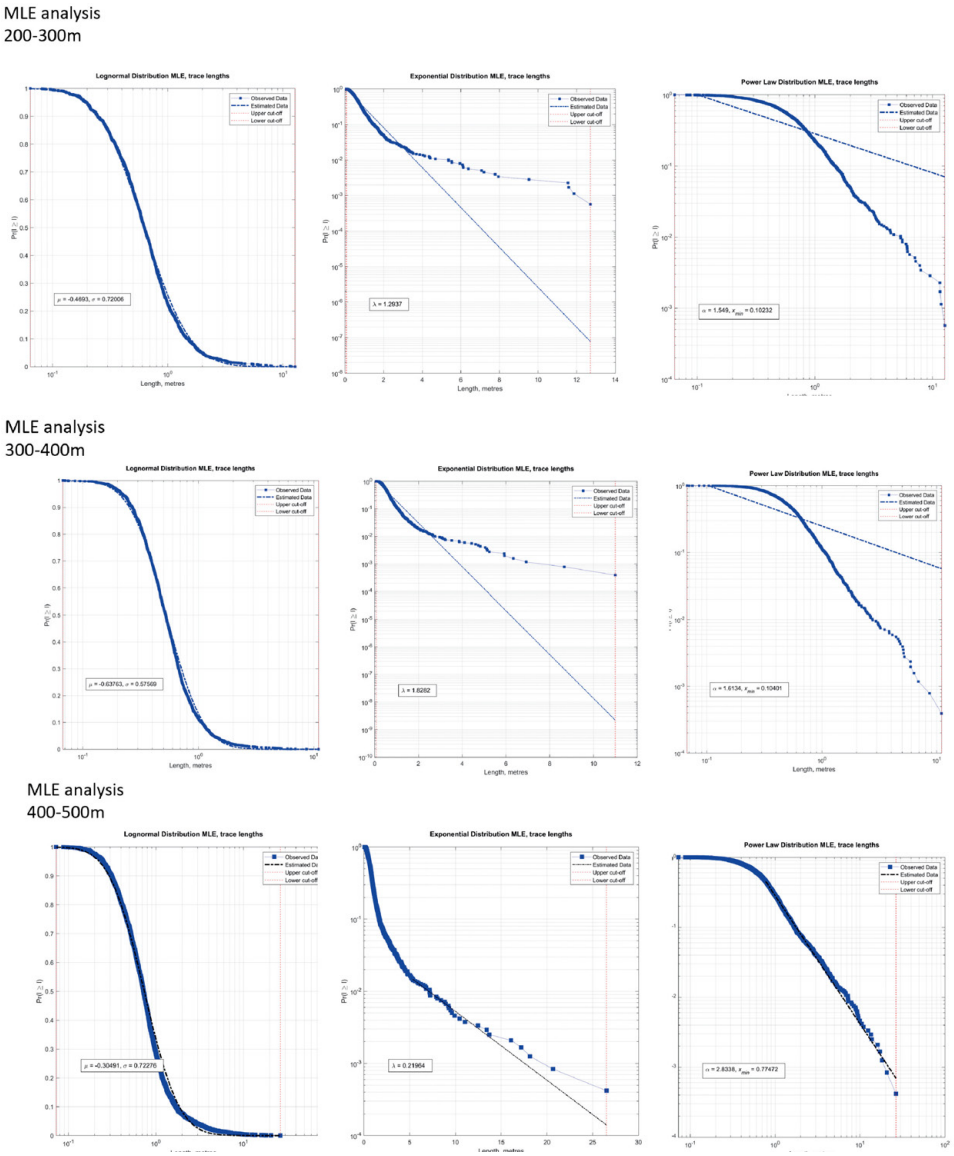

Figure 12 – Maximum likelihood estimator analysis in the exposed quarry wall between 200m and 500m, showing clear tendency towards a lognormal distribution (left) when compared to exponential distribution (middle) and power law distribution (right).

slightly higher near the Southern Fault Zone. This spatial variability in fracture intensity suggests that the southern fault exerts a significant influence on fracture development, potentially enhancing subsurface fluid flow in these regions.

The well-connected fracture networks with regular spacing and log-normal length distributions observed in the Rørdal Quarry are likely to also exist in subsurface chalk reservoirs, forming a key influence on fluid flow and reservoir behaviour. Partitioning of fracture styles between stratigraphic elements of the sequence at Rørdal appears to strongly influence fracture propagation.

Given the scale-dependent fracture growth observed in Rørdal, subsurface models in similar tectonic settings should account for both smaller-scale fractures, which dominate fluid flow, and potential larger-scale fractures, which could contribute significantly to permeability at greater depths. While this study provides valuable insights, further validation with subsurface data is necessary to confirm the relevance of these findings for actual reservoir conditions. Future work should focus on integrating subsurface data, such as well logs or core samples, to refine fracture models and enhance their applicability to subsurface activities such as carbon storage.

8 Concluding Remarks

- The extensive fracture dataset, comprising over 27,400 individual fractures across approximately 7,000 square meters, provides a comprehensive understanding of fracture variations across the Rørdal Quarry, surpassing the detail possible with traditional scan-line and window sampling methods.
- The dataset reveals a bimodal distribution of fracture orientations, with coefficients of variation suggesting clustered patterns, revealing regional fracture trends not previously recognised at the location.

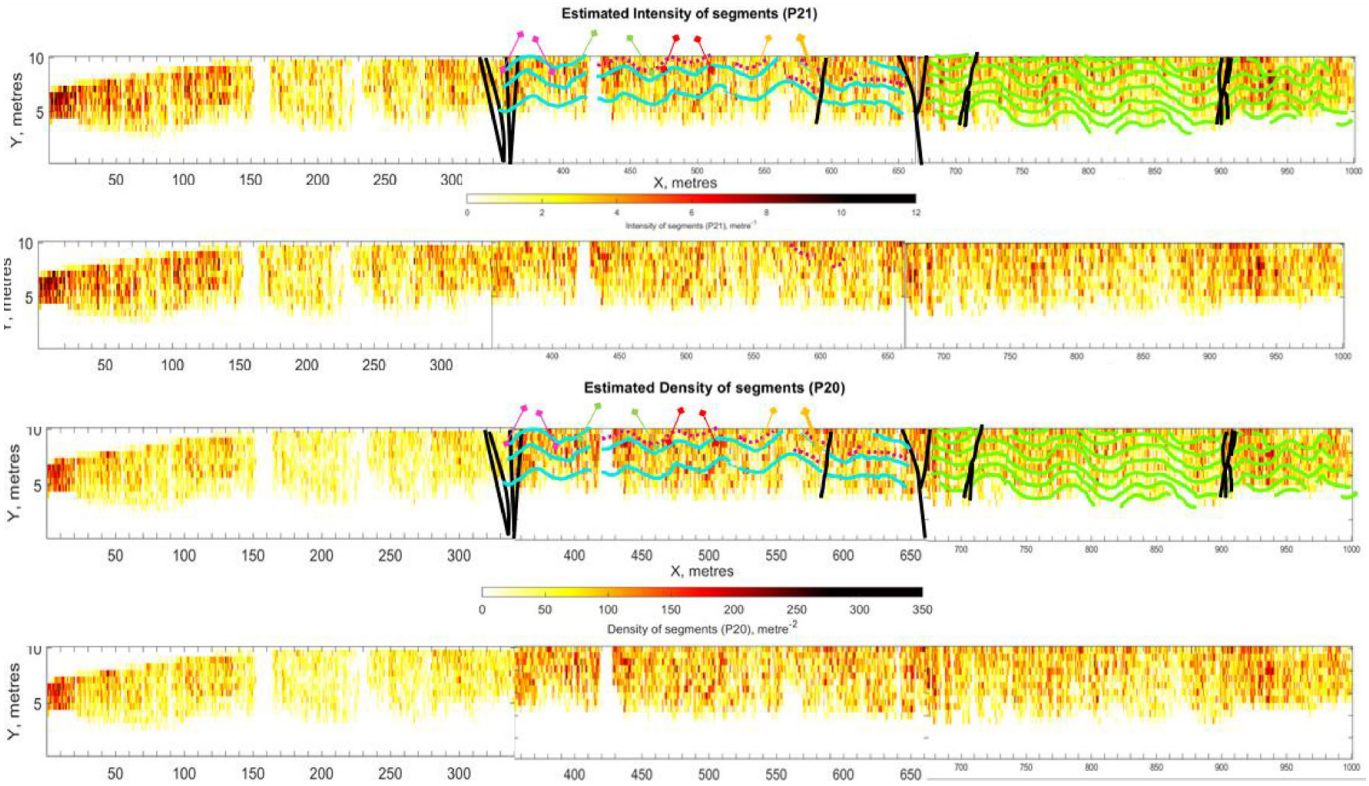

Figure 13 – Intensity (P21) and density (P20) maps from the LQ wall based on fractures mapped on the DOM, generated in FracPaQ using the circular scanline sampling method. Faults are indicated in black and folds are indicated in blue-green within the Sigerslev Member and green in the Rørdal Member.

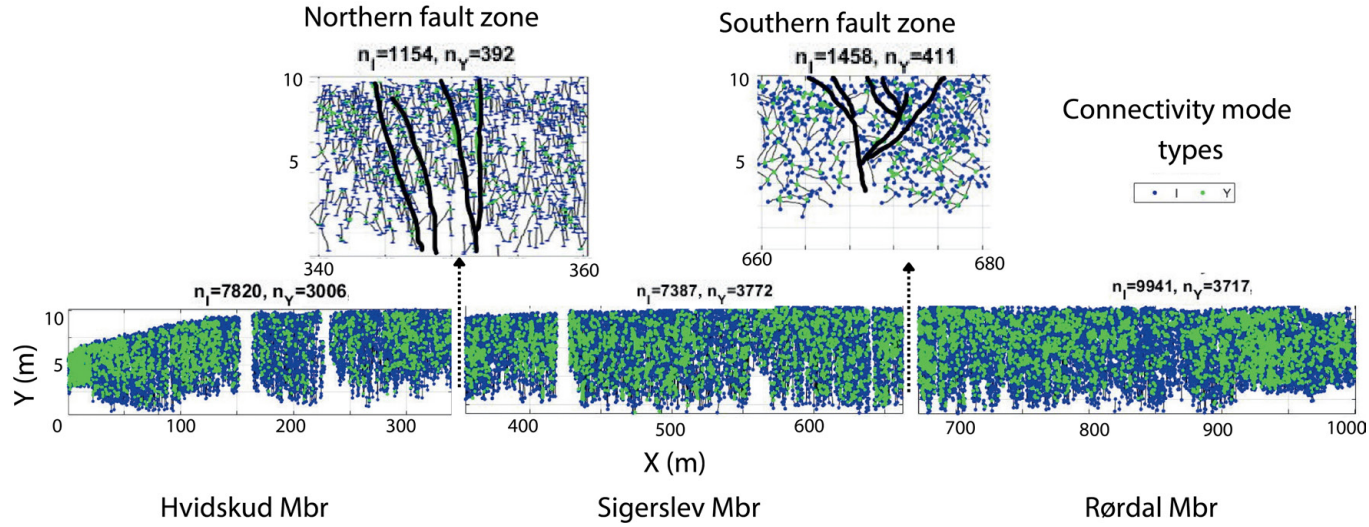

Figure 14 – Isolated (blue) and splay (green) nodes of mapped fracture traces in exposed section, plotted per unit in FracPaQ. I nodes represent isolated ends of traces and y nodes represent branch points. The distribution of I and Y nodes are comparable across the three lithological units, although with a higher degree of connectivity in the northernmost end of the Hvidskud Member.

- The consistency of fracture characteristics, such as main orientations, dip angles, length distributions, and spacing distributions, with those found in other Danish chalk quarries (e.g., Sigerslev, Nye Kløv, Hillerslev) suggests that the these locations are representative more broadly of Upper Cretaceous chalks, supporting the interpretation that these are predominantly layer-bound fracture systems.
- The presence of shallow dipping fractures, likely formed due to glacial-related processes, forms a key difference to offshore reservoirs. Caution should be exercised in removing these fractures from onshore datasets when conditioning subsurface models and interpreters should be aware of their potential impact in cross-cutting earlier fractures.
- This research contributes significantly to understanding natural fracture systems in Upper Cretaceous chalk, reducing reliance on extrapolation from one-dimensional samples from wells and boreholes, which often leads to

inaccuracies in predicting spatial distributions of fracture networks. However, care should be taken when applying these findings to offshore models, particularly considering differences in burial depths and the potential effects of fluid overpressure.

Acknowledgements

The research leading to these results has received funding from the Danish Offshore and Technology Centre under the Advanced Water Flooding program. The authors would like to thank Dr. Michael Welch for his many contributions to discussions and analyses. We would also like to thank Dr. Erik Vest Sørensen, whom has created DOM1A, in which the main fracture data was mapped. Dr. Janina Kammann and Dr. Hemin Yuan are thanked for their work in processing the applied shallow geophysical data. Paul Christiansen is highly thanked for piloting the drone used for imagery data collections of DOMs1B-3B. The Carlsberg Foundation is thanked for funding the DJI drone used for data collection. Additionally, we would like to acknowledge Professor Haakon Fossen and Professor Emeritus Roy Helge Gabrielsen for their valuable insights and constructive feedback during the review process, which significantly enhanced the quality of this work.1B-3B. The Carlsberg Foundation is thanked for funding the DJI drone used for data collection.

Author contributions

TM: Data collection and interpretation (Lead), Investigation (Lead), Methodology (Lead), Conceptualization (Equal), Project administration (Lead), Software (Equal), Validation (Lead), Visualization (Lead), Writing – Original Draft (Lead). **SJO:** Conceptualization (Equal), Software (Equal), Writing – Review & Editing (Supporting). **LS:** Investigation (Supporting), Validation (Supporting), Writing – Review & Editing (Supporting). **LN:** Investigation (Supporting), Validation (Supporting), Writing – Review & Editing (Supporting).

Data availability

All data used for generating figures in this study are available upon request from the corresponding author. The full fracture dataset will be released in an open repository in 2025 for public access.

Competing interests

The authors declare no competing interests.

Peer review

This publication was peer-reviewed by Professor Haakon Fossen and Professor Emeritus Roy Helge Gabrielsen. The full peer-review report can be found here: Review Report.

Copyright notice

References

Aabø, T. M., J. S. Dramsch, C. L. Würtzen, S. Seyum, and M. Welch (2020), An integrated workflow for fracture characterization in chalk reservoirs, applied to the Kraka Field, *Marine and Petroleum Geology*, *112*(104065), 104,065, doi: 10.1016/j.marpetgeo.2019.104065.

Aabø, T. M., S. J. Oldfield, H. Yuan, J. Kammann, E. V. Sørensen, L. Stemmerik, and L. Nielsen (2023), *Geomechanical controls on fracture development in chalk and marl in the Danish North Sea: Understanding and predicting fracture systems*, Springer International Publishing, doi: 10.1007/978-3-031-35327-7.

Anderson, J., and R. Thunvik (1986), Predicting mass transport in discrete fracture networks with the aid of geometrical field data, *Water Resources Research*, *22*, 1941–1950, doi: 10.1029/WR022i013p01941.

Andreo, B., J. Vías, J. J. Durán, P. Jiménez, J. A. López-Geta, and F. Carrasco (2008), Methodology for groundwater recharge assessment in carbonate aquifers: application to pilot sites in southern Spain, *Hydrogeology Journal*, *16*(5), 911–925, doi: 10.1007/s10040-008-0274-5.

Bisdom, K., H. M. Nick, and G. Bertotti (2017), An integrated workflow for stress and flow modelling using outcrop-derived discrete fracture networks, *Computers & Geosciences*, *103*, 21–35, doi: 10.1016/j.cageo.2017.02.019.

Bonnet, E., O. Bour, N. E. Odling, P. Davy, I. Main, P. Cowie, and B. Berkowitz (2001), Scaling of fractures in geological media, *Reviews of Geophysics*, *39*(3), 347–383, doi: 10.1029/1999RG000074.

Bonto, M., M. J. Welch, M. Lüthje, S. I. Andersen, M. J. Veshareh, F. Amour, A. Afrough, R. Mokhtari, M. R. Hajiabadi, M. R. Alizadeh, C. N. Larsen, and H. M. Nick (2021), Challenges and enablers for large-scale CO_2 storage in chalk formations, *Earth-Science Reviews*, *222*(103826), 103,826, doi: 10.1016/j.earscirev.2021.103826.

Boulton, G. S., and P. Caban (1995), Groundwater flow beneath ice sheets: Part II — Its impact on glacier tectonic structures and moraine formation, *Quaternary Science Reviews*, *14*(6), 563–587, doi: 10.1016/0277-3791(95)00058-w.

Cawood, A. J., C. E. Bond, J. A. Howell, R. W. H. Butler, and Y. Totake (2017), LIDAR, UAV or compass-clinometer? Accuracy, coverage and the effects on structural models, *Journal of Structural Geology*, *98*, 67–82, doi: 10.1016/j.jsg.2017.04.004.

Egebjerg Mogensen, T., and J. A. Korstgård (2003), Intra-cratonic dextral transtension and inversion of the southern Kattegat on the southwest margin of Baltica—Seismostratigraphy and structural development, *Tech. rep.*, SGU Research Paper C 832.

Erlström, M., and U. Sivhed (1981), Intra-cratonic dextral transtension and inversion of the southern Kattegat on the southwest margin of Baltica—Seismostratigraphy and

structural development, *Tech. rep.*, SGU Research Paper C 832.

Frykman, P. (2001), Spatial variability in petrophysical properties in Upper Maastrichtian chalk outcrops at Stevns Klint, Denmark, *Marine and Petroleum Geology*, *18*(10), 1041–1062, doi: 10.1016/s0264-8172(01)00043-5.

GEUS (2023), GEUS, https://www.geus.dk, accessed: 2025-1-20.

Gim, D. (2016), CloudCompare: 3D point cloud and mesh processing software.

Healy, D., R. E. Rizzo, D. G. Cornwell, N. J. C. Farrell, H. Watkins, N. E. Timms, E. Gomez-Rivas, and M. Smith (2017), FracPaQ: A MATLAB™ toolbox for the quantification of fracture patterns, *Journal of Structural Geology*, *95*, 1–16, doi: 10.1016/j.jsg.2016.12.003.

Howell, J. A., A. W. Martinius, and T. R. Good (2014), The application of outcrop analogues in geological modelling: a review, present status and future outlook, *Geological Society Special Publication*, *387*(1), 1–25, doi: 10.1144/sp387.12.

Jakobsen, F., and L. Madsen (1996), Report no. 10 Chalk outcrops, North Jutland, Denmark, *Tech. rep.*, Joint Chalk Research Program IV.

Jakobsen, F., and L. Madsen (1997), Faults and joints in chalk, Denmark, *Tech. rep.*, Interim guide to fracture interpretation and flow modelling in fractured reservoirs.

Madsen, L. (1995), Faults and joints in chalk, Denmark, *Tech. rep.*, Interim guide to fracture interpretation and flow modelling in fractured reservoirs.

Nielsen, L., L. O. Boldreel, T. M. Hansen, H. Lykke-Andersen, L. Stemmerik, F. Surlyk, and H. Thybo (2011), Integrated seismic analysis of the Chalk Group in eastern Denmark—Implications for estimates of maximum palaeo-burial in southwest Scandinavia, *Tectonophysics*, *511*(1-2), 14–26, doi: 10.1016/j.tecto.2011.08.010.

Odling, N. E., P. Gillespie, B. Bourgine, C. Castaing, J. P. Chiles, N. P. Christensen, E. Fillion, A. Genter, C. Olsen, L. Thrane, R. Trice, E. Aarseth, J. J. Walsh, and J. Watterson (1999), Variations in fracture system geometry and their implications for fluid flow in fractures hydrocarbon reservoirs, *Petroleum Geoscience*, *5*(4), 373–384, doi: 10.1144/petgeo.5.4.373.

Ortega, O. J., R. A. Marrett, and S. E. Laubach (2006), A scale-independent approach to fracture intensity and average spacing measurement, *AAPG Bulletin*, *90*(2), 193–208, doi: 10.1306/08250505059.

Petrella, E., D. Aquino, F. Fiorillo, and F. Celico (2015), The effect of low-permeability fault zones on groundwater flow in a compartmentalized system. Experimental evidence from a carbonate aquifer (Southern Italy): The effect of low-permeability fault zones on groundwater flow, *Hydrological Processes*, *29*(6), 1577–1587, doi: 10.1002/hyp.10294.

Rizzo, R. E., D. Healy, and L. De Siena (2017), Benefits of maximum likelihood estimators for fracture attribute analysis: Implications for permeability and up-scaling, *Journal of Structural Geology*, *95*, 17–31, doi: 10.1016/j.jsg.2016.12.005.

Rosenbom, A. E., and P. R. Jakobsen (2005), Infrared thermography and fracture analysis of preferential flow in chalk, *Vadose Zone Journal*, *4*(2), 271–280, doi: 10.2136/vzj2004.0074.

Thiele, S. T., L. Grose, A. Samsu, S. Micklethwaite, S. A. Vollgger, and A. R. Cruden (2017), Rapid, semi-automatic fracture and contact mapping for point clouds, images and geophysical data, *Solid Earth*, *8*(6), 1241–1253, doi: 10.5194/se-8-1241-2017.

Thrane, L., and K. Zinck-Jørgensen (1997), Faults and joints in chalk, Denmark: The Thisted Dome, *Tech. rep.*, Geological Survey of Denmark and Greenland (GEUS).

Watkins, H., C. E. Bond, D. Healy, and R. W. H. Butler (2015), Appraisal of fracture sampling methods and a new workflow to characterise heterogeneous fracture networks at outcrop, *Journal of Structural Geology*, *72*, 67–82, doi: 10.1016/j.jsg.2015.02.001.

Welch, M. J., M. Lüthje, and S. J. Oldfield (2020), *Modelling the evolution of natural fracture networks: Methods for simulating the nucleation, propagation and interaction of layer-bound fractures*, Springer International Publishing, doi: 10.1007/978-3-030-52414-2.

Zhang, B., T. Guo, M. Chen, J. Wang, J. Cao, H. Wang, and Z. Qu (2024), Effect of bedding planes and property contrast between layers on the propagation mechanism of hydraulic fracture height in shale reservoirs, *Computers and Geotechnics*, *175*(106715), 106,715, doi: 10.1016/j.compgeo.2024.106715.

Ziegler, P. A. (1990), *Geological Atlas of Western and Central Europe, 2nd edition*, 239 pp., Shell Internationale Petroleum Maatschappij B.V.